Supplementary Material

Anthropogenic CO2, air-sea CO2 fluxes and acidification in the Southern Ocean: results from a time-series analysis at station OISO-KERFIX (51°S-68°E).

Nicolas Metzl[1], Claire Lo Monaco[1], Coraline Leseurre[1,2], Céline Ridame[1], Gilles Reverdin[1], Thi Tuyet Trang Chau[3], Frédéric Chevallier[3], Marion Gehlen[3]

1 Laboratoire LOCEAN/IPSL, Sorbonne Université-CNRS-IRD-MNHN, Paris, 75005, France

2 Flanders Marine Institute (VLIZ), 8400 Ostend, Belgium

3 Laboratoire LSCE/IPSL, CEA-CNRS-UVSQ, Université Paris-Saclay Gif-sur-Yvette, 91191, France

Correspondence to: Nicolas Metzl (nicolas.metzl@locean.ipsl.fr)

This document includes Tables S1-S5 and Figures S1-S18 providing the supplementary information that supports part of the discussion presented in the main article.

Table S1a: List of stations occupied at OISO-KERFIX location (50°40'S-68°25'E) with A_T-C_T data used in this analysis. * indicates data from GLODAP data product version v2021 (Lauvset et al, 2021). Cruises OISO-21 to OISO-31 will be available in version GLODAP-V3. PI stands for Principal Investigator.

Cruise	Ship	Year	Month	Day	PI
INDIGO *	Marion Dufresne I	1985	3	13	A. Poisson
KERFIX *	La Curieuse	1992	5	1	A. Poisson/C. Jeandel
KERFIX *	La Curieuse	1992	7	3	A. Poisson/C. Jeandel
KERFIX *	La Curieuse	1992	9	17	A. Poisson/C. Jeandel
KERFIX *	La Curieuse	1992	10	16	A. Poisson/C. Jeandel
KERFIX *	La Curieuse	1992	11	24	A. Poisson/C. Jeandel
KERFIX *	La Curieuse	1992	12	17	A. Poisson/C. Jeandel
KERFIX *	La Curieuse	1992	12	17	A. Poisson/C. Jeandel
KERFIX *	La Curieuse	1993	1	30	A. Poisson/C. Jeandel
KERFIX *	La Curieuse	1993	4	6	A. Poisson/C. Jeandel
KERFIX *	La Curieuse	1993	5	15	A. Poisson/C. Jeandel
KERFIX *	La Curieuse	1993	6	10	A. Poisson/C. Jeandel
KERFIX *	La Curieuse	1993	7	16	A. Poisson/C. Jeandel
KERFIX *	La Curieuse	1993	8	17	A. Poisson/C. Jeandel
KERFIX *	La Curieuse	1993	9	16	A. Poisson/C. Jeandel
KERFIX *	La Curieuse	1993	10	27	A. Poisson/C. Jeandel
KERFIX *	La Curieuse	1993	11	28	A. Poisson/C. Jeandel
OISO-01 *	Marion Dufresne II	1998	2	3	N.Metzl
OISO-02 *	Marion Dufresne II	1998	8	26	N.Metzl
OISO-03 *	Marion Dufresne II	1998	12	15	N.Metzl
OISO-03 *	Marion Dufresne II	1998	12	15	N.Metzl
OISO-04 *	Marion Dufresne II	2000	1	24	N.Metzl
OISO-05 *	Marion Dufresne II	2000	7	31	N.Metzl
OISO-06 *	Marion Dufresne II	2001	1	13	N.Metzl
OISO-08 *	Marion Dufresne II	2002	1	14	N.Metzl
OISO-11 *	Marion Dufresne II	2004	2	2	N.Metzl
OISO-12 *	Marion Dufresne II	2005	2	10	N.Metzl
OISO-18 *	Marion Dufresne II	2010	1	13	C.Lo Monaco/N.Metzl
OISO-19 *	Marion Dufresne II	2011	1	30	C.Lo Monaco/N.Metzl
OISO-21	Marion Dufresne II	2012	2	9	C.Lo Monaco/N.Metzl
OISO-22	Marion Dufresne II	2013	2	24	C.Lo Monaco/N.Metzl
OISO-24	Marion Dufresne II	2015	1	21	C.Lo Monaco/N.Metzl
OISO-25	Marion Dufresne II	2016	1	14	C.Lo Monaco/N.Metzl
OISO-26	Marion Dufresne II	2016	10	18	C.Lo Monaco/N.Metzl
OISO-27	Marion Dufresne II	2017	1	22	C.Lo Monaco/N.Metzl
OISO-28	Marion Dufresne II	2018	1	21	C.Lo Monaco/N.Metzl
OISO-29	Marion Dufresne II	2019	1	26	C.Lo Monaco/N.Metzl
OISO-30	Marion Dufresne II	2020	1	20	C.Lo Monaco/N.Metzl
OISO-31	Marion Dufresne II	2021	2	15	C.Lo Monaco/N.Metzl

Table S1b: List of cruises extracted from SOCAT data product version v2022 (Bakker et al, 2022) in the region around 50°S-68°E. For some cruises when there is no measured salinity or when salinity is suspected we used the salinity from World Ocean Atlas (WOA) also available in SOCAT data files (Pfeil et al, 2013; Antonov et al, 2006). PI stands for Principal Investigator.

Expocode	Ship	PI	Salinity	Cruises Flag SOCAT
31AR19620519	Argo	Keeling, C. D.	WOA	D
35MF19910105	Marion Dufresne I	Poisson, A.		D
35MF19910224	Marion Dufresne I	Poisson, A.		D
35MF19910413	Marion Dufresne I	Poisson, A.		D
35MF19910728	Marion Dufresne I	Poisson, A.		D
35MF19920414	Marion Dufresne I	Poisson, A.	WOA	D
35MF19920725	Marion Dufresne I	Poisson, A.	WOA	D
35MF19930130	Marion Dufresne I	Poisson, A.		D
74E319930210	Discovery	Robertson, J.		D
35MF19930319	Marion Dufresne I	Poisson, A.	WOA	D
35MF19930330	Marion Dufresne I	Poisson, A.	WOA	D
35MF19930524	Marion Dufresne I	Poisson, A.		D
35MF19930625	Marion Dufresne I	Poisson, A.		D
35MF19940128	Marion Dufresne I	Metzl, N.		E
35MF19950928	Marion Dufresne I	Metzl, N.	WOA	D
35MF19980121	Marion Dufresne II	Metzl, N.		D
35MF19980819	Marion Dufresne II	Metzl, N.		D
35MF19981204	Marion Dufresne II	Metzl, N.		D
35MF20000115	Marion Dufresne II	Metzl, N.		D
35MF20000721	Marion Dufresne II	Metzl, N.		D
35MF20010104	Marion Dufresne II	Metzl, N.		D
35MF20020105	Marion Dufresne II	Metzl, N.		D
35MF20040106	Marion Dufresne II	Metzl, N.		D
35MF20050113	Marion Dufresne II	Metzl, N.		D
35MF20050919	Marion Dufresne II	Metzl, N.		D
35MF20060105	Marion Dufresne II	Metzl, N.		D
35MF20070104	Marion Dufresne II	Metzl, N.		D
35MF20080105	Marion Dufresne II	Metzl, N.		D
35MF20091224	Marion Dufresne II	Metzl, N.		D
35MF20110115	Marion Dufresne II	Metzl, N.		D
35MF20111011	Marion Dufresne II	Metzl, N.		D
35MF20120125	Marion Dufresne II	Metzl, N.		D
35MF20130210	Marion Dufresne II	Metzl, N.		D
35MF20140109	Marion Dufresne II	Metzl, N.: Lo Monaco, C.		B
35MF20150107	Marion Dufresne II	Metzl, N.: Lo Monaco, C.		B
35MF20160108	Marion Dufresne II	Metzl, N.: Lo Monaco, C.		B
35MV20161006	Marion Dufresne II	Metzl, N.: Lo Monaco, C.		B
35MV20170105	Marion Dufresne II	Metzl, N.: Lo Monaco, C.		B
35MV20180105	Marion Dufresne II	Lo Monaco, C.: Metzl, N.		B
35MV20190109	Marion Dufresne II	Lo Monaco, C.: Metzl, N.		B
35MV20200106	Marion Dufresne II	Lo Monaco, C.: Metzl, N.		B
35MV20210113	Marion Dufresne II	Lo Monaco, C.: Metzl, N.		B

Table S2: Mean values and standard error (Std) of properties in deep water (> 1450m) observed in 1985-2021 at station OISO-KERFIX (50°40'S-68°25'E). Results for C_T and A_T are shown in Figure S1. pH, $[H^+]$, $[CO_3^{2-}]$, Ω_{Ca}, Ω_{Ar} and C_{ant} calculated as described in the manuscript. NB is the number of data selected in the layer. Only data with WOCE/GLODAP flag 2 selected (e.g. C_T data in 2014 discarded).

	θ (°C)	S PSU	O_2 $\mu M.kg^{-1}$	A_T $\mu M.kg^{-1}$	C_T $\mu M.kg^{-1}$	pH TS	$[H^+]$ $nM.kg^{-1}$	$[CO_3^{2-}]$ $\mu M.kg^{-1}$	Ω_{Ca}	Ω_{Ar}	C_{ant} $\mu M.kg^{-1}$
Mean	1.653	34.758	203.0	2349.2	2240.7	7.910	12.3	84.7	1.463	0.938	6.5
Std	0.075	0.004	3.6	4.2	3.7	0.012	0.4	2.3	0.038	0.025	5.4
NB	44	42	42	41	43	40	40	40	40	40	39

Figures S1: Time-series of C_T and A_T concentrations observed in deep water (> 1450m) in 1985-2021 at station OISO-KERFIX (50°40'S-68°25'E). The mean values and standard-error for all cruises (Table S2) indicated by dashed-black and dashed-grey lines. Accuracy data is ± 3 $\mu mol.kg^{-1}$ (vertical bars).

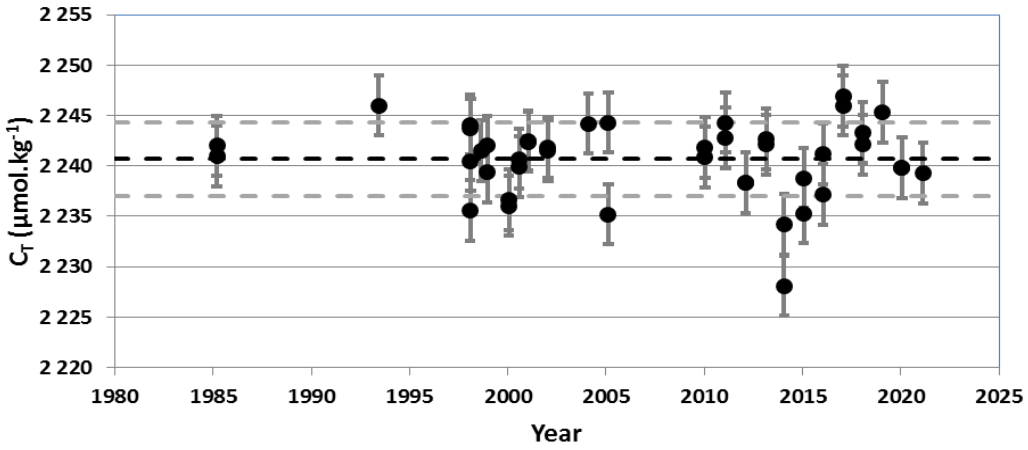

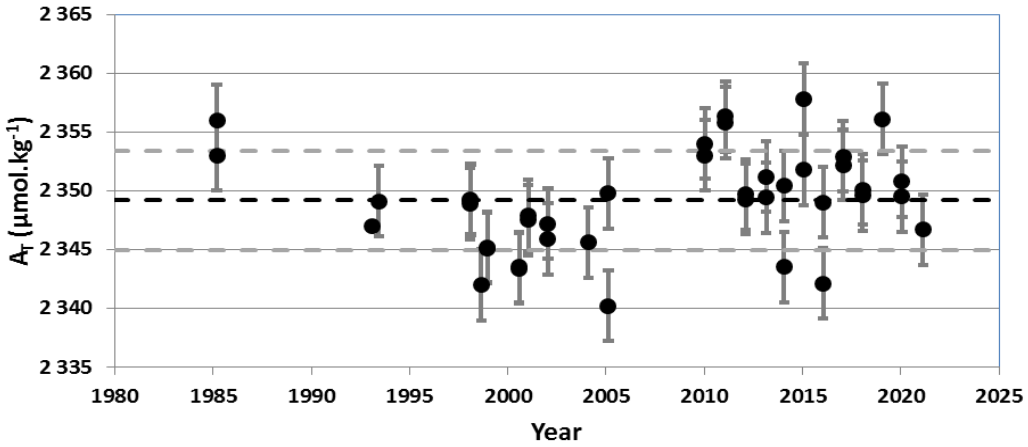

Comparison of measured and calculated properties for different data-sets:

To validate the carbonate properties calculated with different data-sets, we compare the surface properties used for the trend analysis. Table S3 presents the difference between measured underway fCO_2 data with those derived from the FFNN model for 1991-2020. Table S4 presents the differences between Station data (based on A_T-C_T measurements) with properties calculated from the fCO_2 data or from the FFNN data for all cruises in 1991-2021. Finally, in Table S5 we compare FFNN data for March 1985 with the data at that station for the same period (INDIGO cruise).

Table S3: Mean difference (DIFF) and standard-deviation (STD) of properties derived from the surface fCO_2 data-set and the FFNN model at location 50.5°S-68.5°E. For the period 1991 to 2020 we identified 35 months for this comparison. Figure S2 shows the time-series for observed and modeled fCO_2 and their differences.

	SST (°C)	SAL PSU	A_T $\mu M.kg^{-1}$	C_T $\mu M.kg^{-1}$	fCO_2 µatm	pH TS	$[H^+]$ $nM.kg^{-1}$	$[CO_3^{2-}]$ $\mu M.kg^{-1}$	Ω_{Ca}	Ω_{Ar}	Revelle
DIFF	-0.063	0.004	0.4	1.5	2.1	-0.002	0.049	-0.7	-0.019	-0.012	0.054
STD	(0.360)	(0.068)	(4.9)	(5.0)	(7.0)	(0.008)	(0.148)	(2.1)	(0.050)	(0.032)	(0.145)

Table S4: Mean difference and standard-deviation (STD) of properties derived from the underway surface fCO_2 data or the FFNN model with observations in the Mixed-Layer. For the period 1993 to 2021 we identified 22 co-located months for this comparison (21 for the FFNN model). Figure S3 shows the results for C_T.

Data	SST °C	SAL PSU	A_T $\mu M.kg^{-1}$	C_T $\mu M.kg^{-1}$	fCO_2 µatm	pH TS	$[H^+]$ $nM.kg^{-1}$	$[CO_3^{2-}]$ $\mu M.kg^{-1}$	Ω_{Ca}	Ω_{Ar}	Revelle
fCO2	-0.010	-0.009	-5.1	-8.2	-8.7	0.008	-0.160	1.6	0.036	0.023	-0.141
(STD)	(0.189)	(0.062)	(6.2)	(6.5)	(10.6)	(0.012)	(0.224)	(2.6)	(0.063)	(0.039)	(0.177)
FFNN	-0.116	-0.011	-4.5	-6.2	-6.4	0.006	-0.108	0.7	0.013	0.008	-0.074
(STD)	(0.403)	(0.034)	(5.0)	(7.2)	(14.9)	(0.016)	(0.315)	(4.2)	(0.099)	(0.063)	(0.291)

Figure S2: (a): Time-series of fCO_2 (µatm) data from observations in 1991-2021 (grey circles) near station OISO-KERFIX (50°40'S-68°25'E) and from the FFNN model (black diamonds) for the same months and location. (b): Time-series of the differences between observed fCO_2 and the FFNN model. The mean differences and associated standard-deviations for all cruises (Table S3) are indicated respectively by dashed-black and dashed-grey lines. In both figures the vertical bars are the standard deviations of observed fCO_2 in the box 50°S-51.5°S/67.5-69°E (see Figure 1, Yellow Square). As opposed to the fCO_2 data (top, figure S2a) there is no trend in the calculated differences (bottom, figure S2b). The same is observed for all properties listed in Table S3.

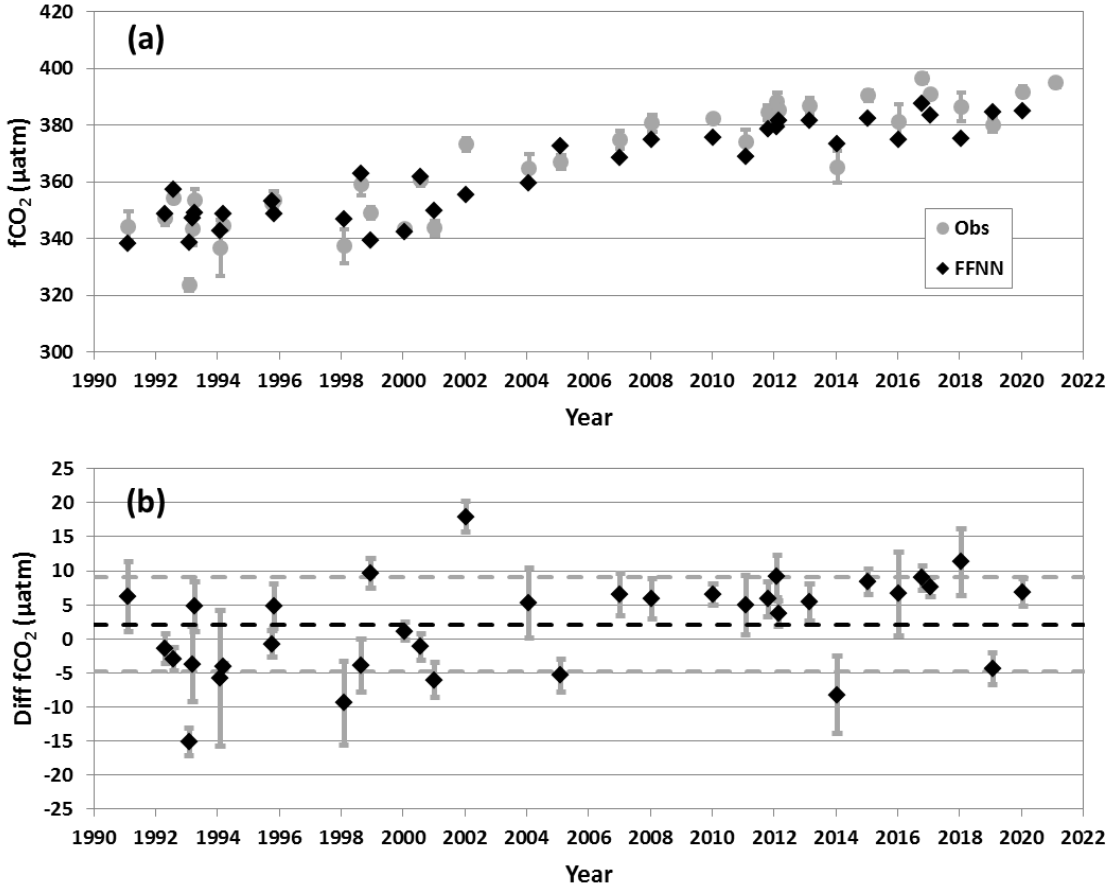

Figure S3: (a): Time-series of C_T (µmol.kg^{-1}) data from observations in 1991-2021 (CT-STAT, orange triangles) at station OISO-KERFIX (50°40'S-68°25'E) and C_T calculated from the surface fCO_2 dataset (grey circle) or from the FFNN model (black diamond) for the same months. Vertical bars are the standard deviation of C_T measurements or as observed in the box 50°S-51.5°S/67.5-69°E (see Figure 1). (b): Time-series of the differences between observed C_T in the mixed-layer and calculated C_T from the surface fCO_2 dataset or the FFNN model. There is no trend in the calculated differences (bottom figure) and the same is observed for all properties listed in Table S4 (not shown).

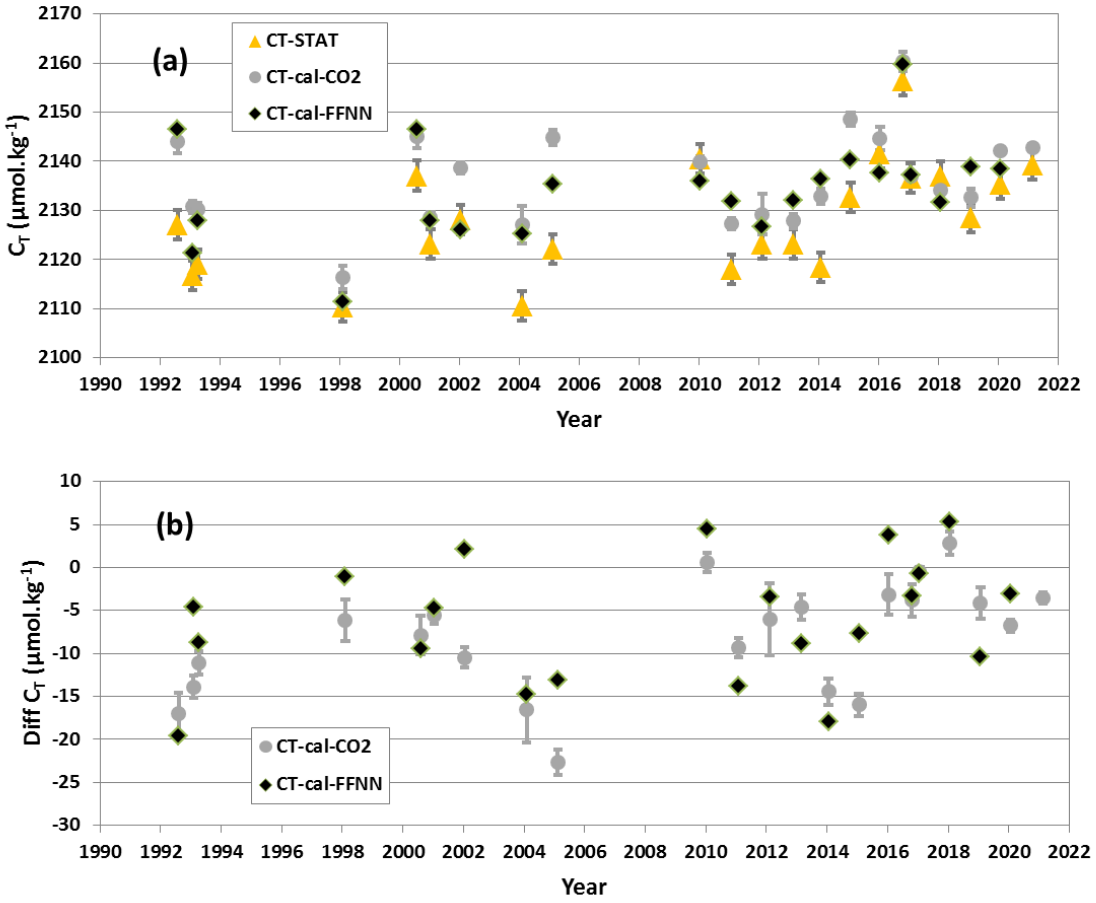

Table S5: Mean properties measured (Temperature, salinity, A_T and C_T) or calculated in March 1985 at Station INDIGO-16 (50.5°S/67.27°E) in the mixed-layer (3 samples in the layer 0-75m) and the same properties based on the FFNN model at the surface for the same period (March 1985). Standard deviations of data are in bracket and differences (FFNN-Data) also listed. Figure S4 shows the seasonal cycle of the SST, C_T, fCO_2 and pH for 1985.

	TEMP °C	SAL PSU	A_T $\mu M.kg^{-1}$	C_T $\mu M.kg^{-1}$	fCO_2 µatm	pH TS	$[H^+]$ $nM.kg^{-1}$	Ω_{Ca}	Ω_{Ar}
INDIGO Cruise	4.734 (0.002)	33.873 (0.017)	2286.7 (1.5)	2119.3 (1.2)	336.8 (1.0)	8.101 (0.002)	7.916 (0.039)	2.883 (0.021)	1.817 (0.013)
FFNN Model	4.906	33.802	2281.5	2115.2	339.5	8.100	7.936	2.907	1.831
Difference	0.172	-0.071	-5.1	-4.1	2.7	-0.001	0.020	0.024	0.014

Figure S4: Seasonal cycle of sea surface temperature, C_T, fCO_2 and pH from the FFNN model in 1985 (black or grey diamonds) and observations from INDIGO-16 station (50.5°S/67.27°E) in March 1985 (black and grey triangles). The atmospheric fCO_2 in 1985 is also shown (red-dashed line) indicating the region was a CO_2 source in March to October. This validates the analysis of the trends based on FFNN model starting in 1985.

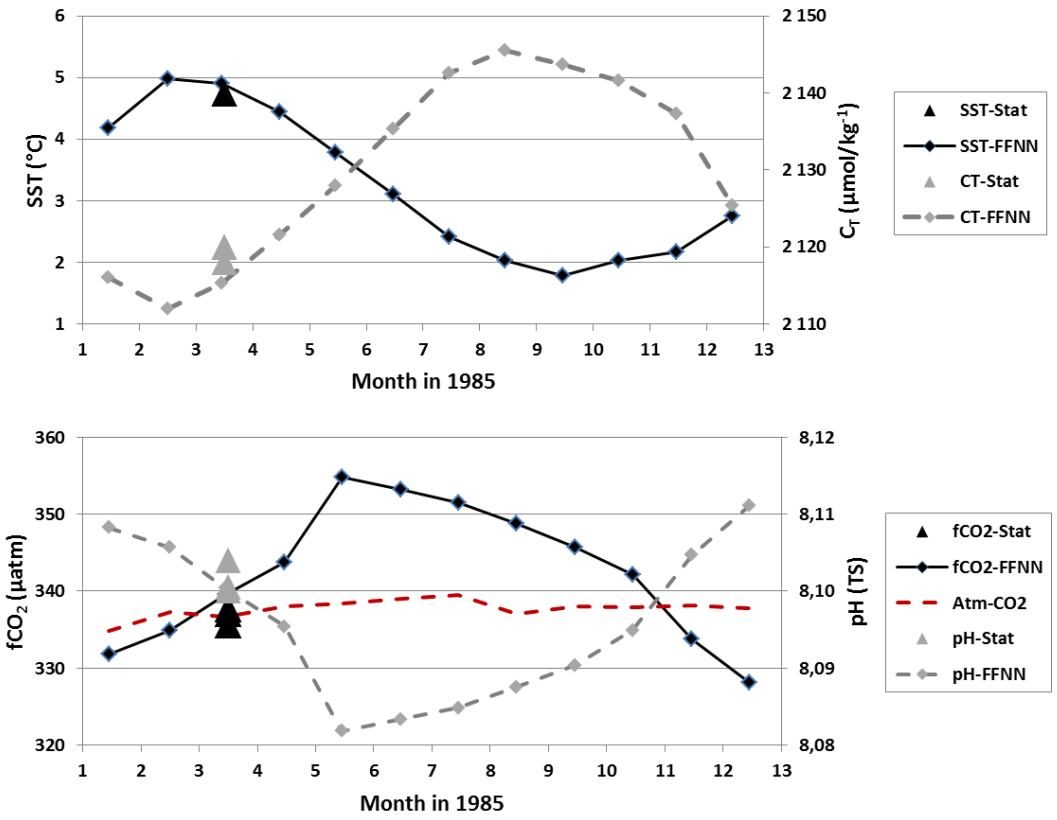

Figure S5: Time-series of A_T and C_T (µmol.kg^{-1}) measured in 1992-2021 in January-February (red) and October (black) in the mixed-layer (0-30m) at station OISO-KERFIX (50°40'S-68°25'E).

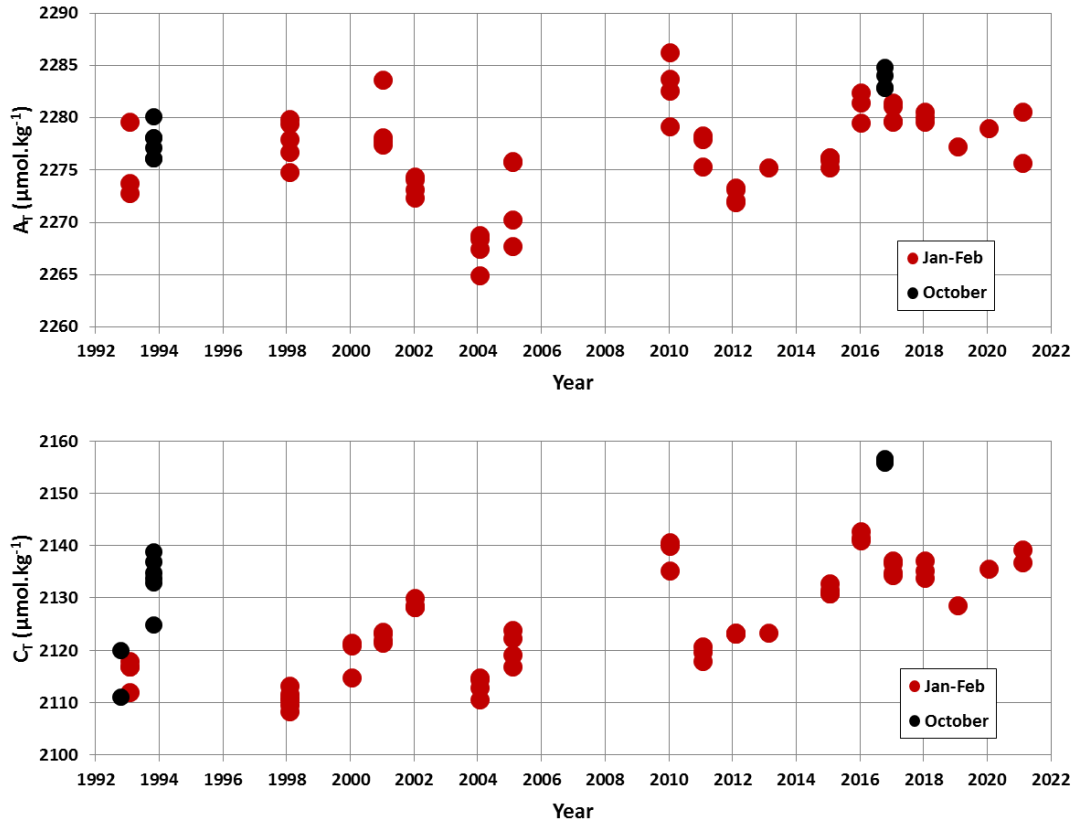

Figure S6: (a): Time-series of Silicate concentrations (SIL, µmol.kg^{-1}) measured in January-February 1998-2021 in the mixed-layer (0-30m) at station OISO-10 (50°40'S-68°25'E). (b): Hovmoller section of Silicate in the layer 0-150m in January-February 1998-2021. Silicate concentrations were particularly low in 1998, 2014 and 2016 (down to 100m) and high in 2002 and 2020. Section produced with ODV (Schlitzer, 2018).

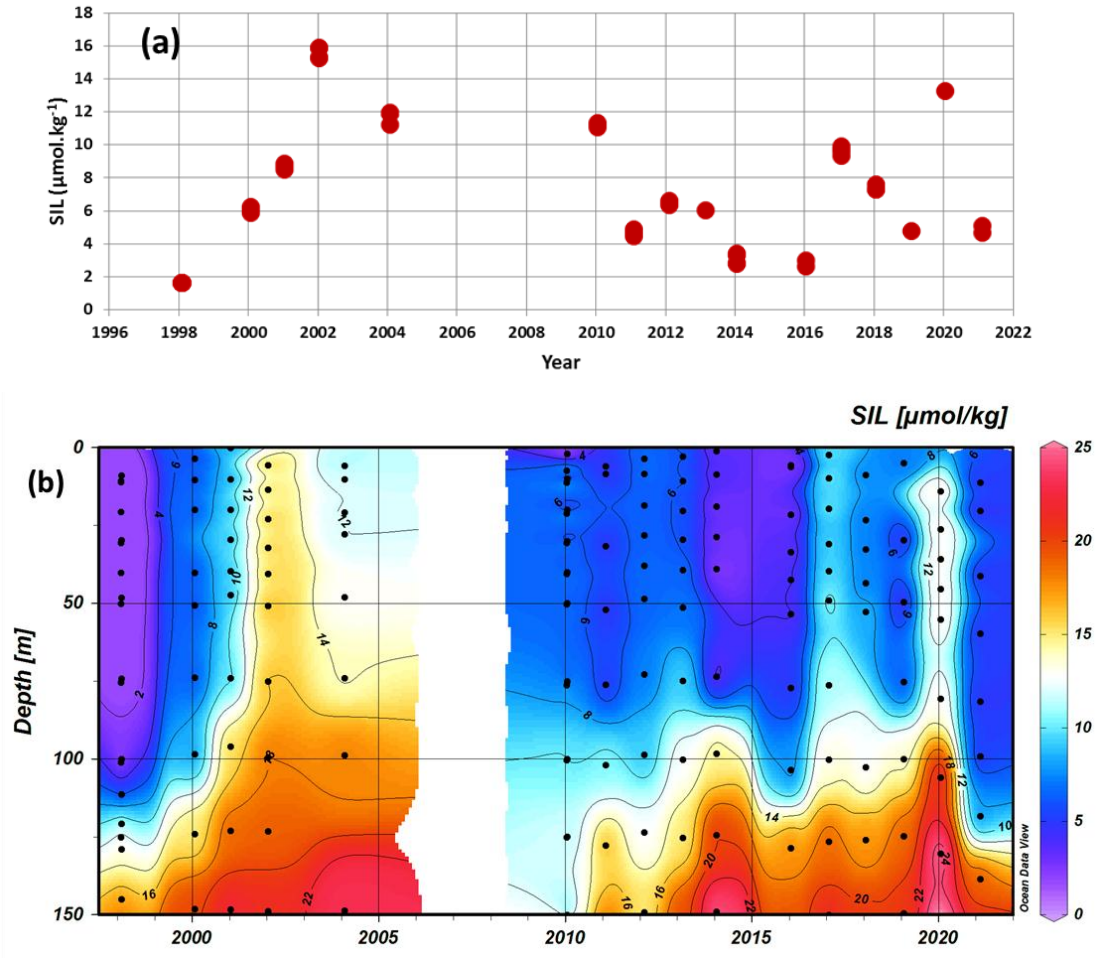

Figure S7: (a) Time-series (1998-2021) of sea surface Chl-a ($mg.m^{-3}$) from weekly satellite data (SeaWIFS and MODIS, triangles) and from in-situ data in the layer 0-20m at station OISO-10 (circles, red for January, blue for August and black for October). Due to cloud cover there is no satellite data during austral winter. (b): same Chl-a time-series for the period 2012-2016 highlighting the Chl-a cycle in austral summer 2014 and 2016 that explains the low fCO_2 compared to 2013 or 2015 (see Figure 2 and S8).

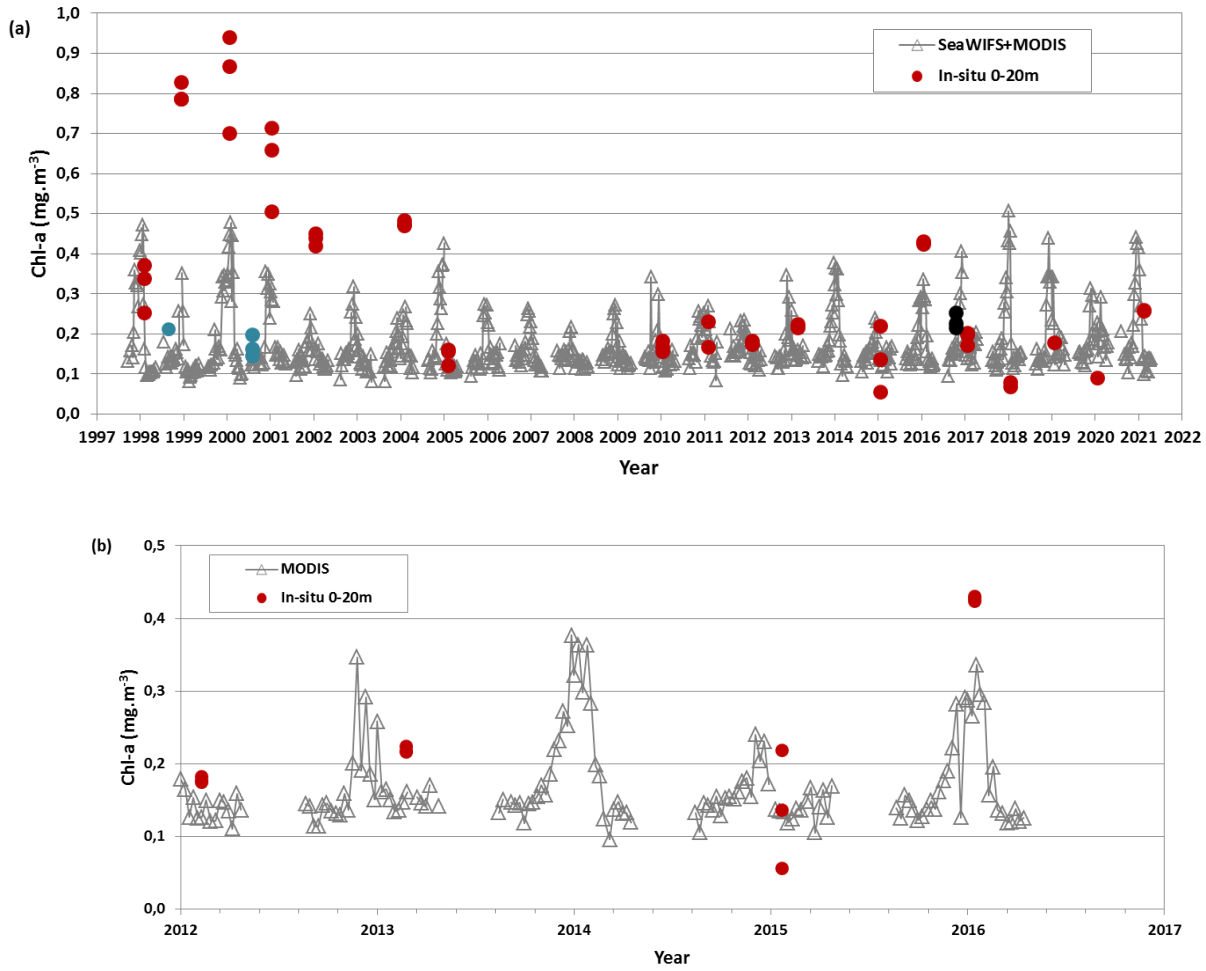

Figure S8: Mean oceanic fCO_2 (µatm) observed in 2010-2020 in January-February (grey circle) and from the FFNN model in January (purple diamonds) close to station OISO-10 (50°40'S-68°25'E). Atmospheric fCO_2 is also shown (red line). In summer both observed and modeled oceanic fCO_2 trends of less than +1 µatm.yr^{-1} are much lower than the atmospheric fCO_2 rate of +2.37 µatm.yr^{-1} for this period. The low oceanic fCO_2 trend in summer is likely linked to an increase in primary production as suggested from Chl-a records (Figure 5).

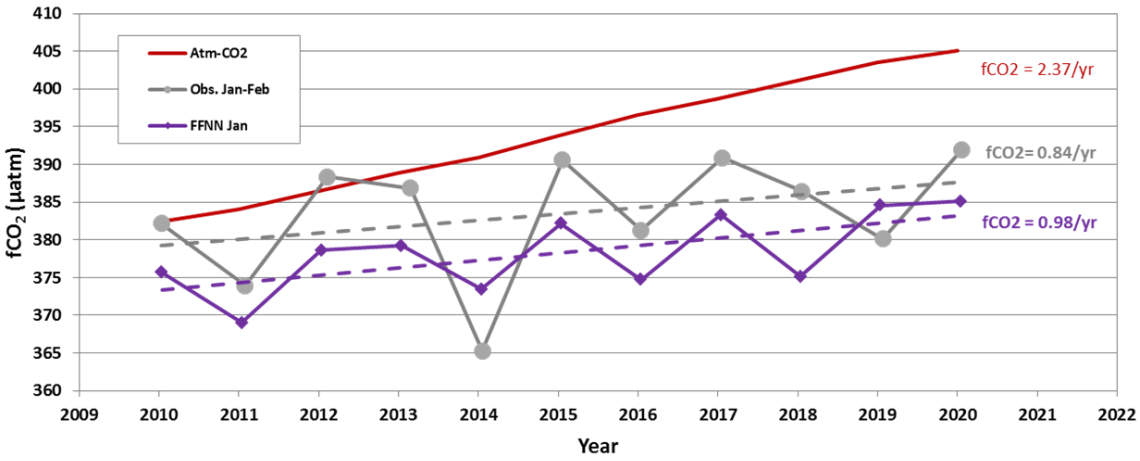

Figure S9: (a): Time-series (1991-2021) of sea surface temperature (SST in °C) from monthly data (grey symbols, Reynolds et al, 2002) and observed in-situ in January-February (red circles) at location 50.5°S-67.5°E. The 12 months running mean (black line) highlights the inter-annual variability and the progressive cooling in 2018-2021. (b): Detail of SST in 2018-2021. The dashed lines identify the trends from the monthly SST (-0.474 ± 0.164 °C.yr^{-1}) or from observed SST in summer (-0.253 ± 0.092 °C.yr^{-1}).

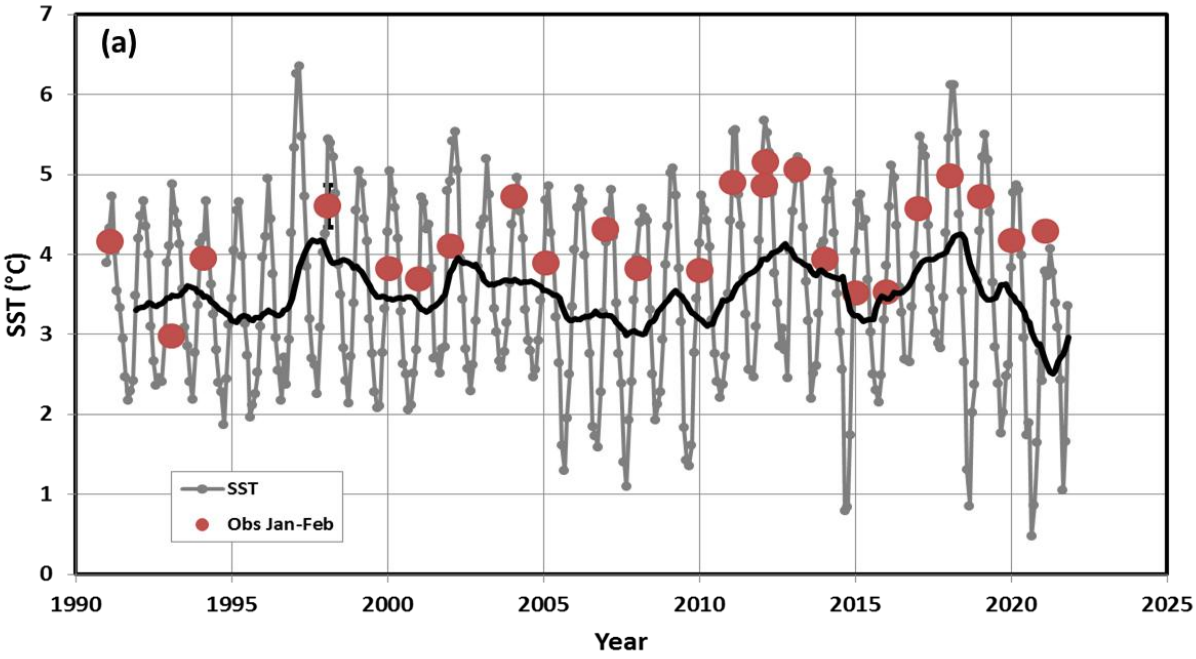

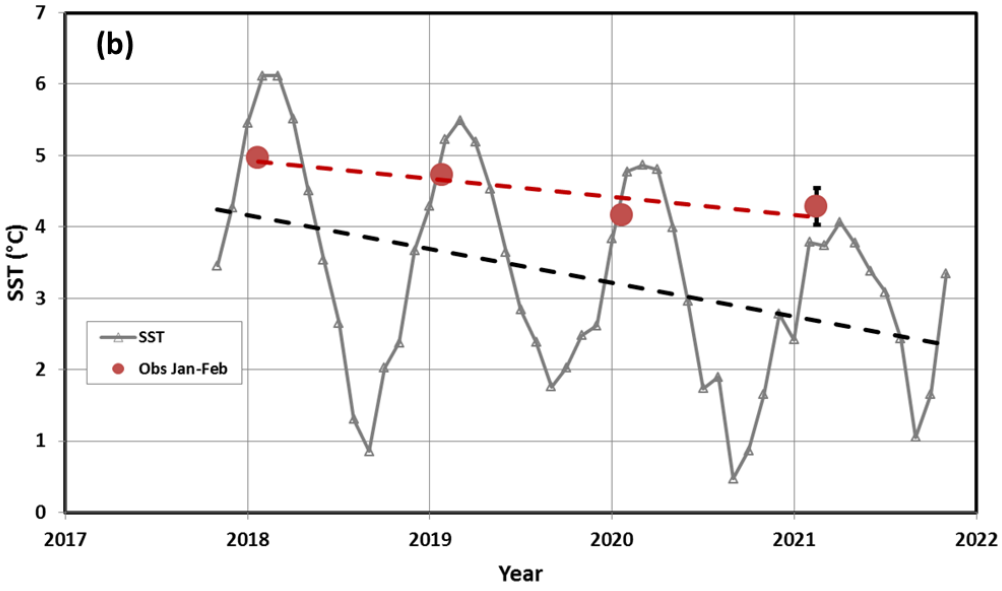

Figure S10: Hovmoller sections of C_T and O_2 (µmol.kg^{-1}) at station OISO-KERFIX (50°40'S-68°25'E) in 1985-2021. The O_2 minimum (< 180 µmol.kg^{-1}) is observed in the layer 600-800m. Sections produced with ODV (Schlitzer, 2018).

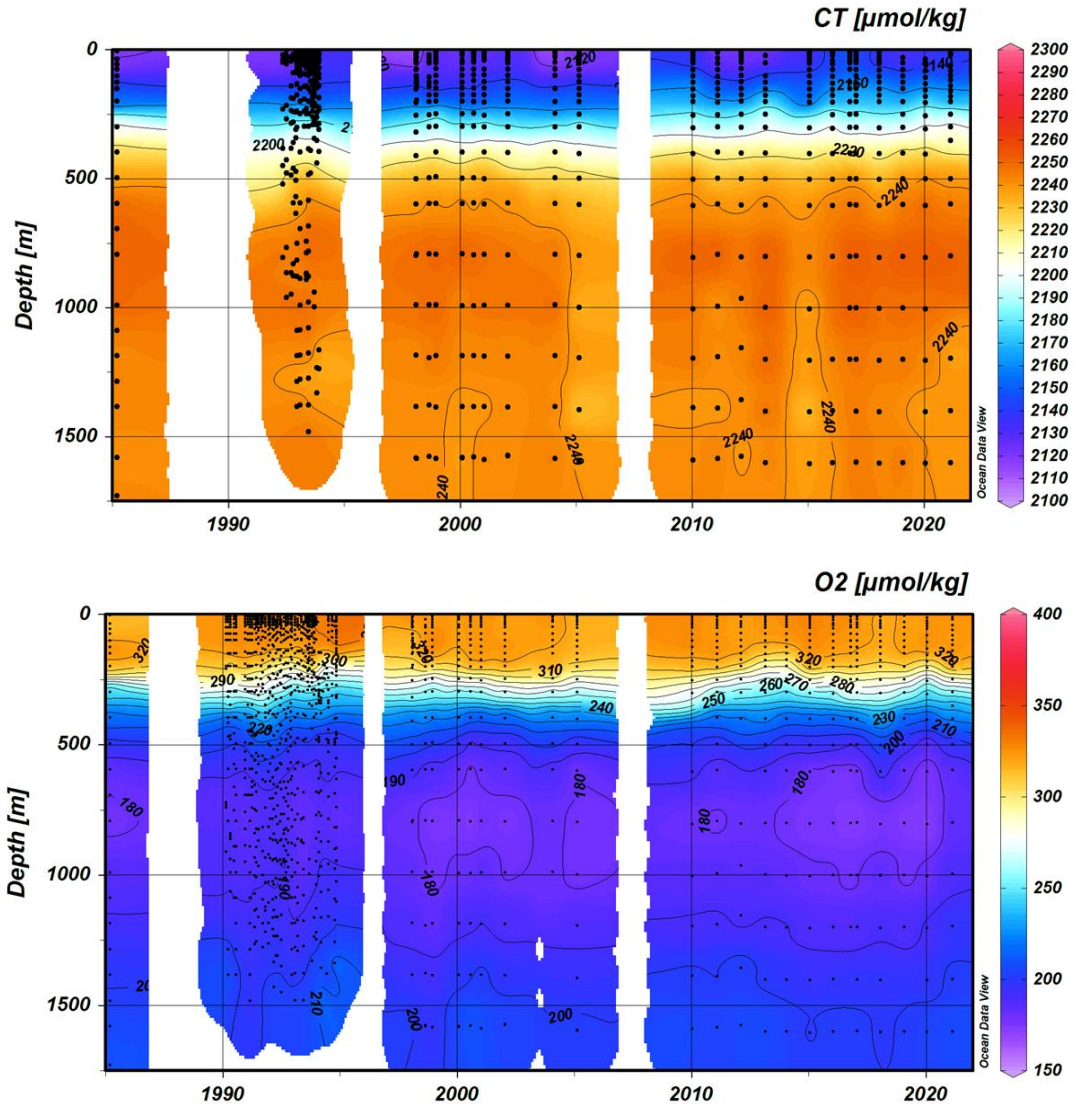

Figure S11: Comparisons of C_{ant} concentrations (µmol.kg^{-1}) and potential temperature (°C) profiles in austral winter 1998, 2000 and 2016 (black symbols) and the following summer (red symbols) at station OISO-10 (50°40'S-68°25'E). In the WW layer (temperature minimum around 200m) the C_{ant} in summer is almost equal to the C_{ant} evaluated in the mixed-layer during winter. For summer the C_{ant} values in surface layer 0-150m are not shown (the method is not applicable in the productive zone).

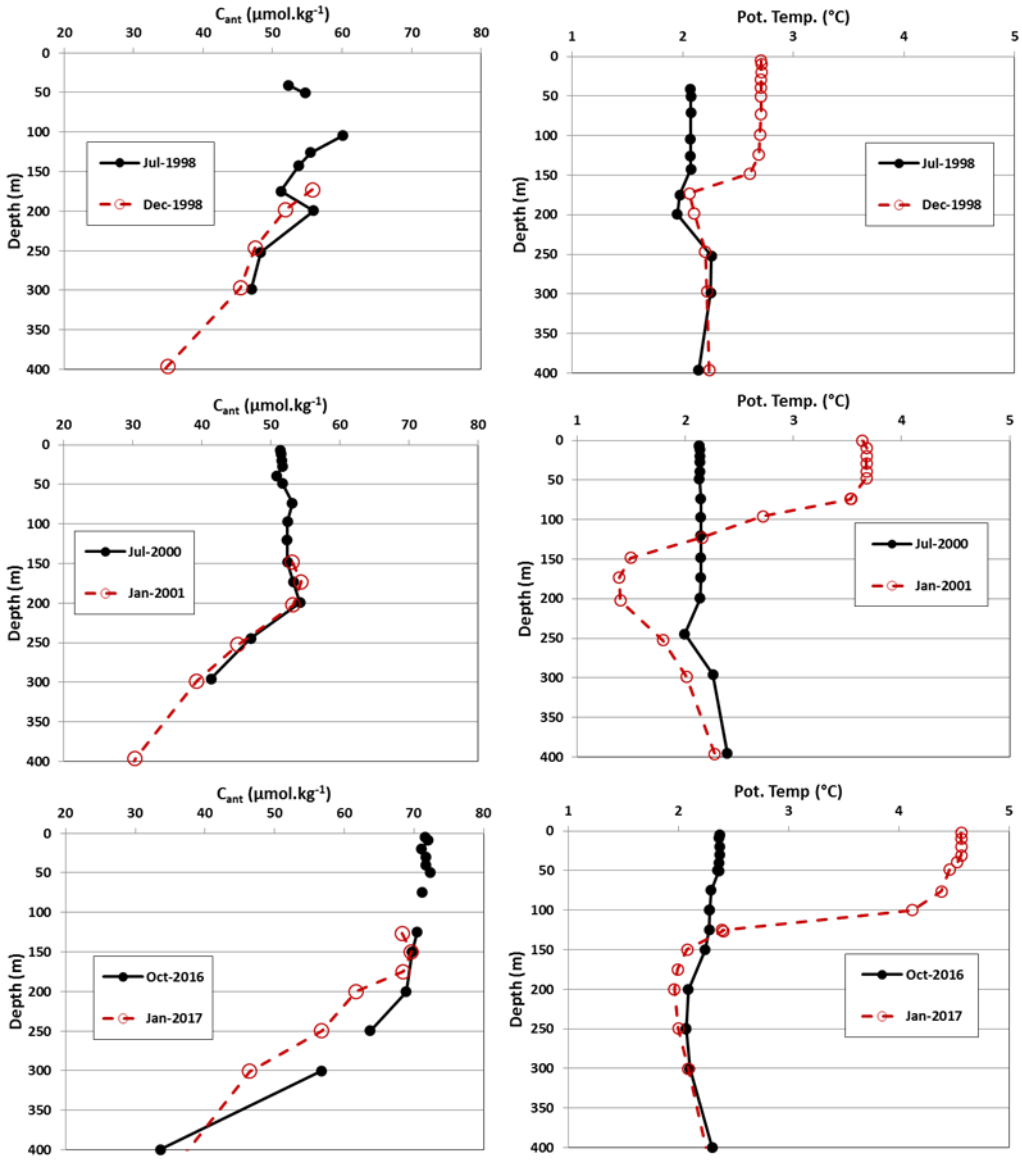

Figure S12: (a): Time-series and trends of sea surface C_T ($\mu mol.kg^{-1}.yr^{-1}$) for different season based on observations (for January, red circles) and the FFNN model (for January or August) around station at 50°40'S-68°25'E in 1985-2021. The trends for C_T are indicated for January (+0.68 ± 0.05 $\mu mol.kg^{-1}.yr^{-1}$ red dashed) and August (+055 ± 0.04 $\mu mol.kg^{-1}.yr^{-1}$ blue dashed). The time-series of C_{ant} ($\mu mol.kg^{-1}.yr^{-1}$) in the WW is also shown (black circles, right axis). (b): Time-series and trends of sea surface C_T ($\mu mol.kg^{-1}.yr^{-1}$) from the FFNN model in January for the periods 1985-2001, 2001-2010 and 2010-2020. (c): Time-series of sea surface C_T ($\mu mol.kg^{-1}$) in January (red) or August (blue) from the FFNN model in 2010-2020 compared to C_T (dashed) due only to the C_{ant} accumulation after 2010. In August the increase of C_T is mainly explained by C_{ant}. In summer C_T is lower compared to the C_T due to C_{ant}.

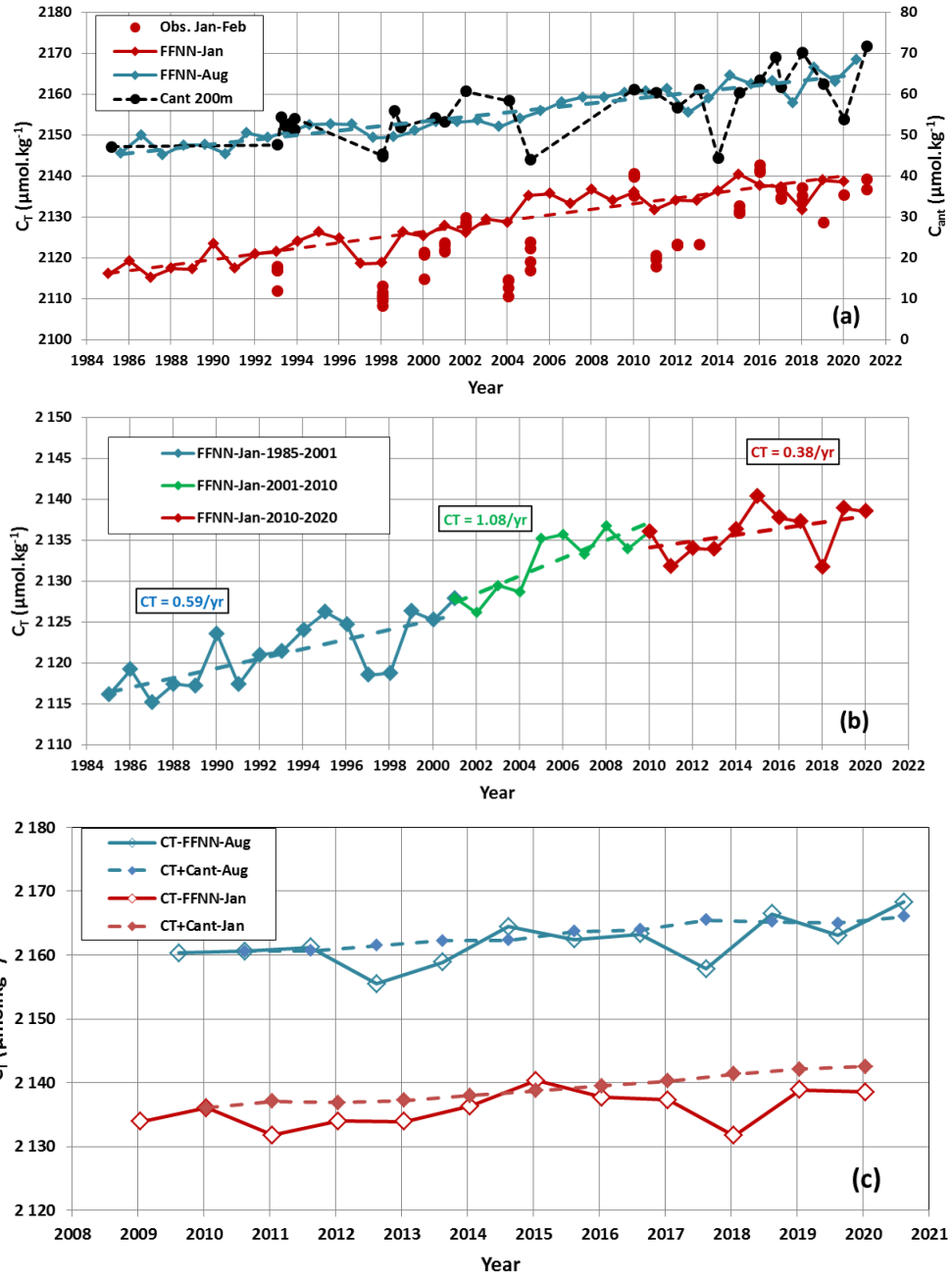

Figure S13: (a): Time-series of $[H^+]$ surface concentrations (nmol.kg^{-1}) around station OISO-KERFIX at 50°40'S-68°25'E calculated from fCO_2 data (Figure 2) using the A_T/S relation (see text). The color dots correspond to 5 seasons (January-February, March-April, July-August, October and December) and triangles the average for each period. The monthly sea surface $[H^+]$ from the FFNN model is presented for the period 1985-2020 (purple line). The annual $[H^+]$ trend in 1985-2020 of +0.0324 nmol.kg^{-1}.yr^{-1} (± 0.0007) (dashed purple) is derived from the FFNN monthly data. (b): Trends of $[H^+]$ (nmol.kg^{-1}.yr^{-1}) for different seasons and periods based on observations (January) and the FFNN model (January or August). (c): Profiles (0-400m left axis) of $[H^+]$ at station OISO-KERFIX in March 1985, January 2020 and January 2021 along with surface time-series in 1985-2020 (right axis) in January (yellow line) and August (blue line) from the FFNN model.

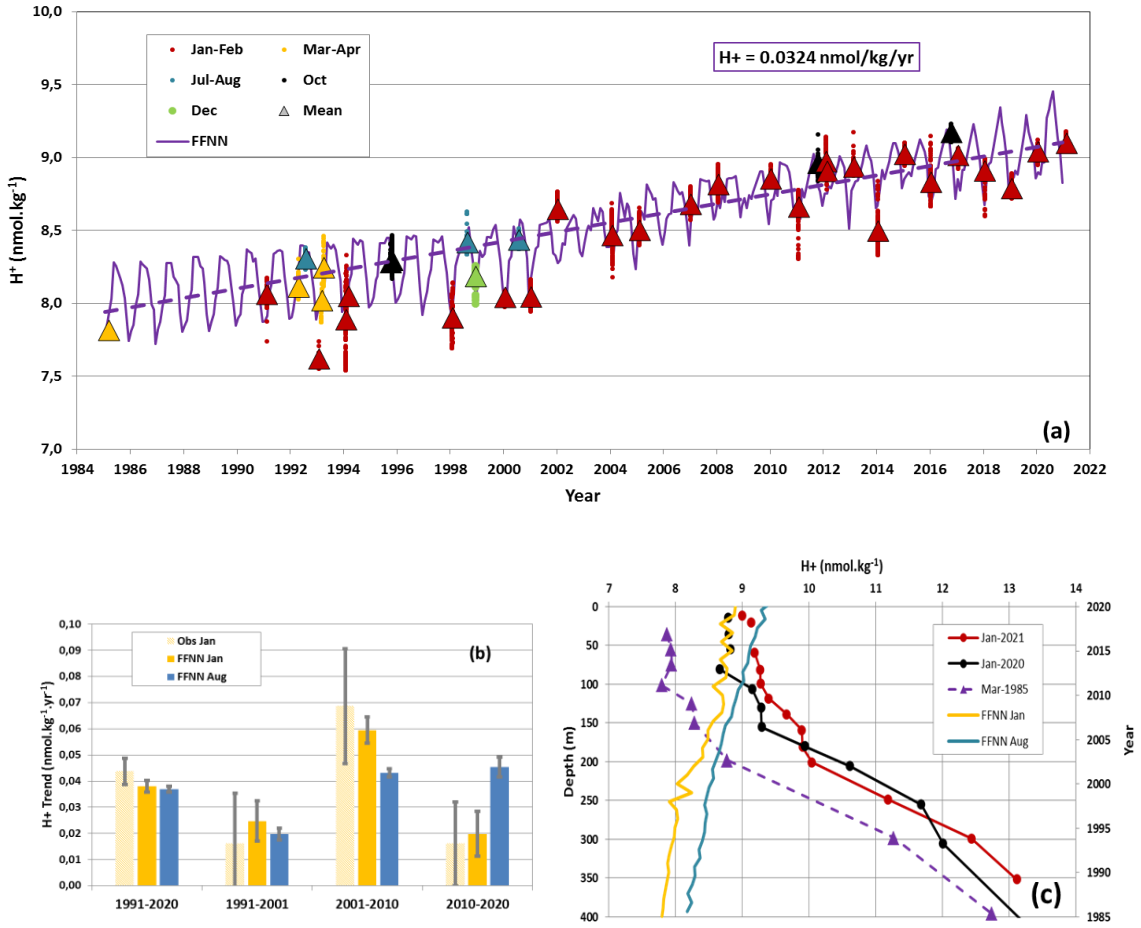

Figure S14: Hovmoller section (Depth-Time) of pH, [CO_3^{2-}] concentrations (µmol.kg^{-1}) and Ω_{Ar} in 1985-2021 at station OISO-KERFIX (50°40'S-68°25'E). The sections are presented in the layer 0-800m. The [CO_3^{2-}] minimum is around 600m. Sections produced with ODV (Schlitzer, 2018).

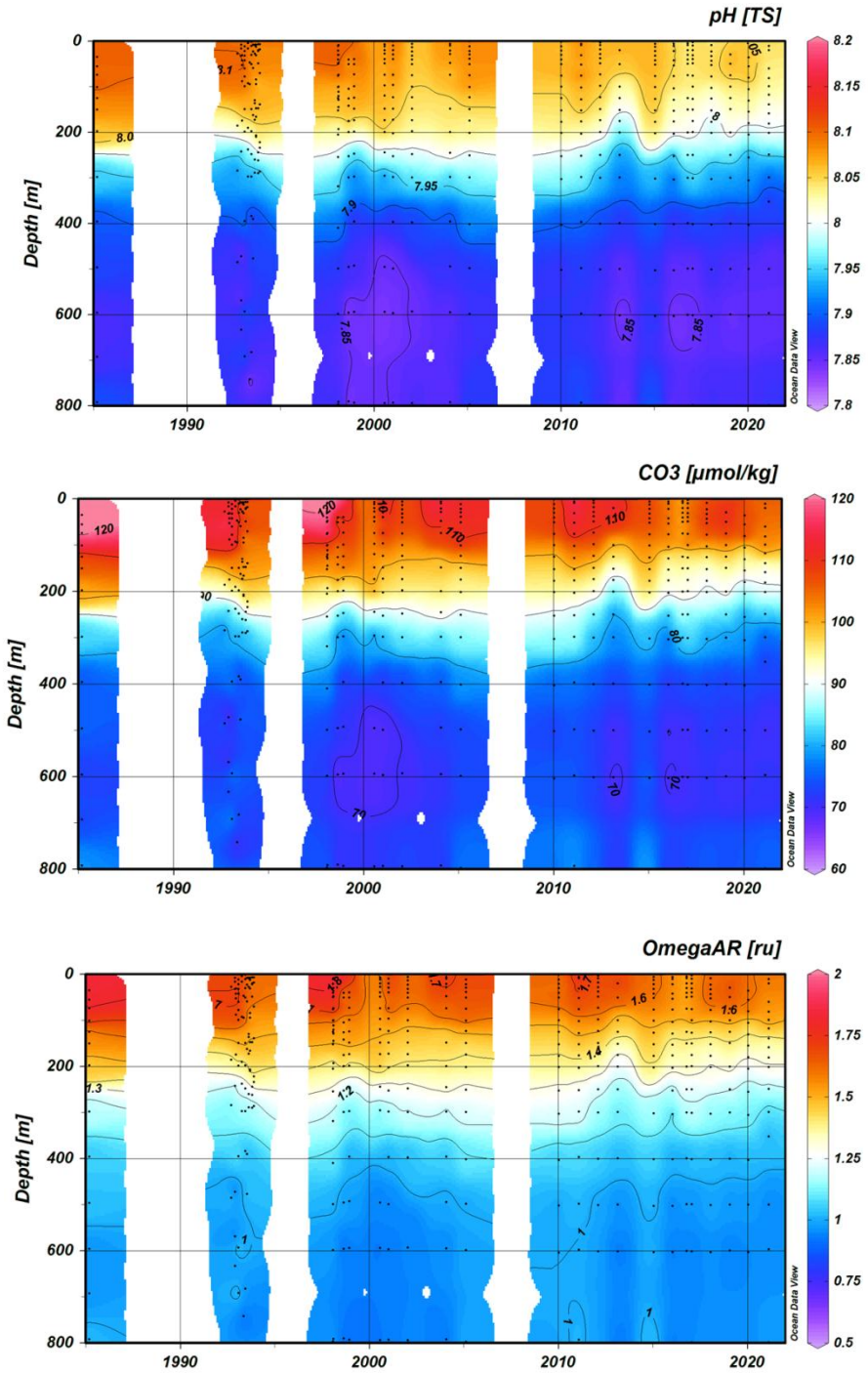

Figure S15: Profiles of C_{ant}, $[CO_3^{2-}]$, Ω_{Ar} and Ω_{Ca} for present days and pre-industrial (PI) periods based on March 1985 data (black symbols) and February 2021 data (red symbols) at station OISO-KERFIX (50°40'S-68°25'E). Pre-industrial values are calculated when C_{ant} is subtracted to C_T for each sample (PI profiles are shown below 150m only, C_{ant} not available in surface layer). The $[CO_3^{2-}]$ minimum lies around 600m and decreased by 10 µmol.kg^{-1} from pre-industrial to present days. Ω_{Ar} at 1 is found at the bottom (1600m) for pre-industrial, below 600m in 1985 and below 400m in 2021. Note that the pre-industrial $[CO_3^{2-}]$ and Ω profiles are very similar either using 1985 or 2021 data.

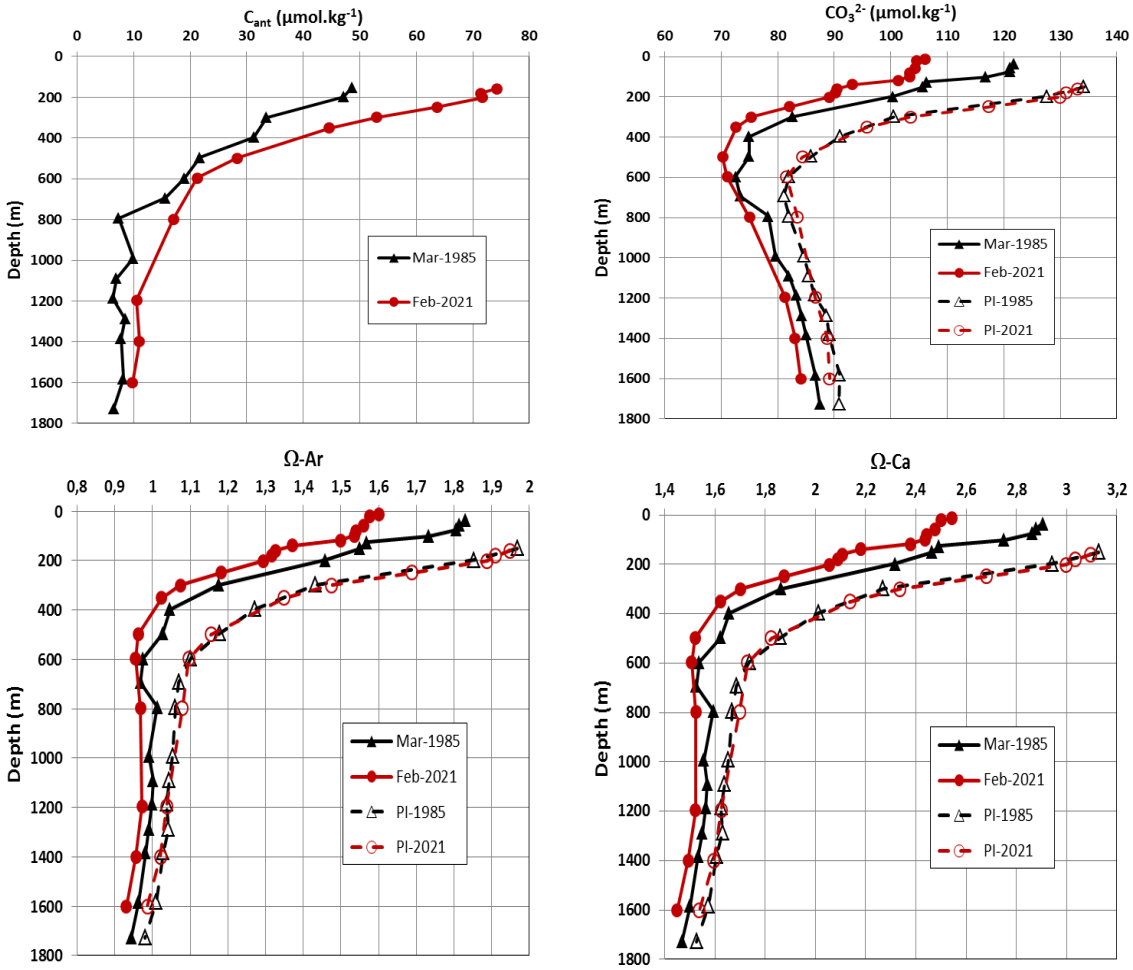

Figure S16: Comparisons of Ω_{Ar} profiles in austral winter 1998, 2000 and 2016 (black symbols) and the following summer (red symbols) at station OISO-10 (50°40'S-68°25'E). Below 200m (winter water, WW) there is no change of Ω_{Ar} from one season to the next. For these periods the under-saturation (Ω_{Ar} <1) is always below 400m.

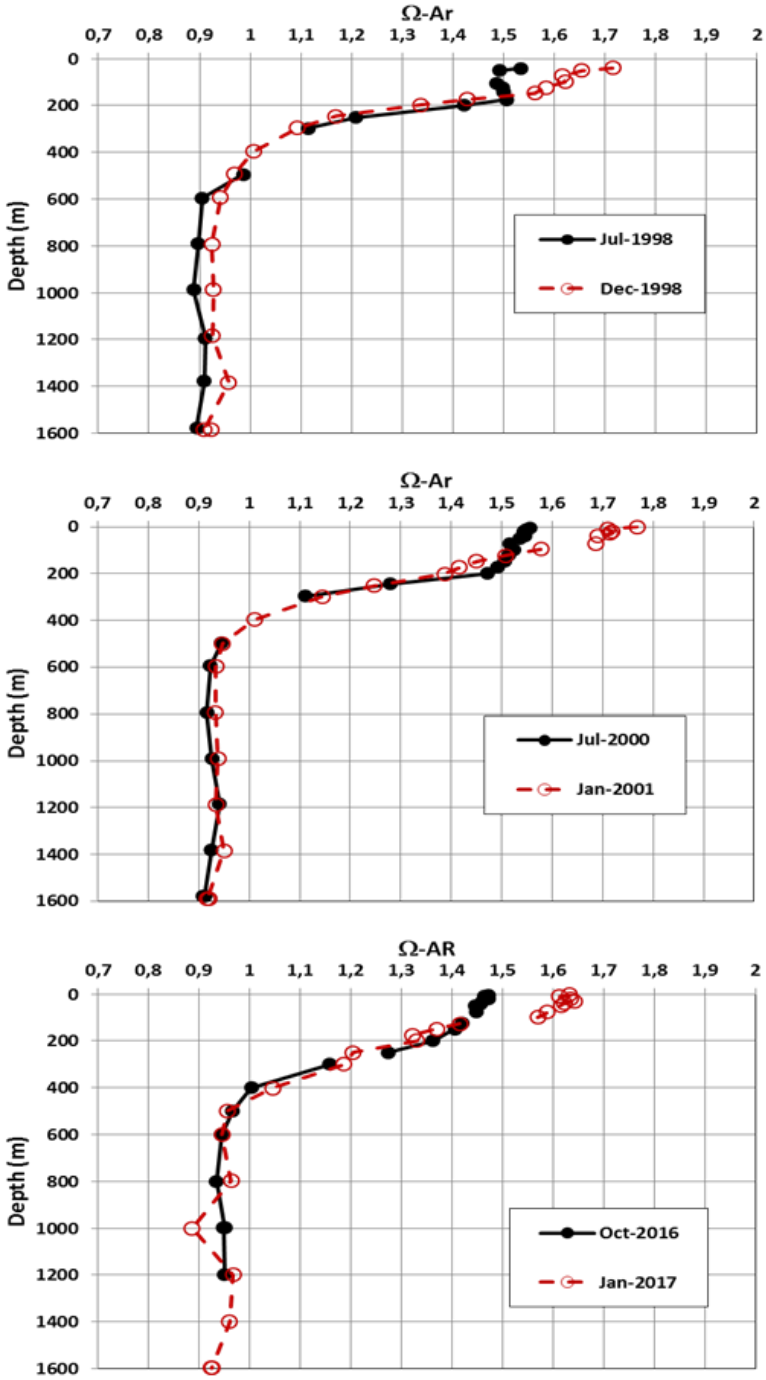

Figure S17: Evolution of pH, $[H^+]$ ($nmol.kg^{-1}$) and Ω_{Ar} in austral winter (blue) and summer (red) around station OISO-KERFIX (50°40'S-68°25'E) from the FFNN model. Here the trends for 1985-2020 are extrapolated in time. The saturation (Ω_{Ar}=1) would be reached at year 2110 in winter and 2120 in summer.

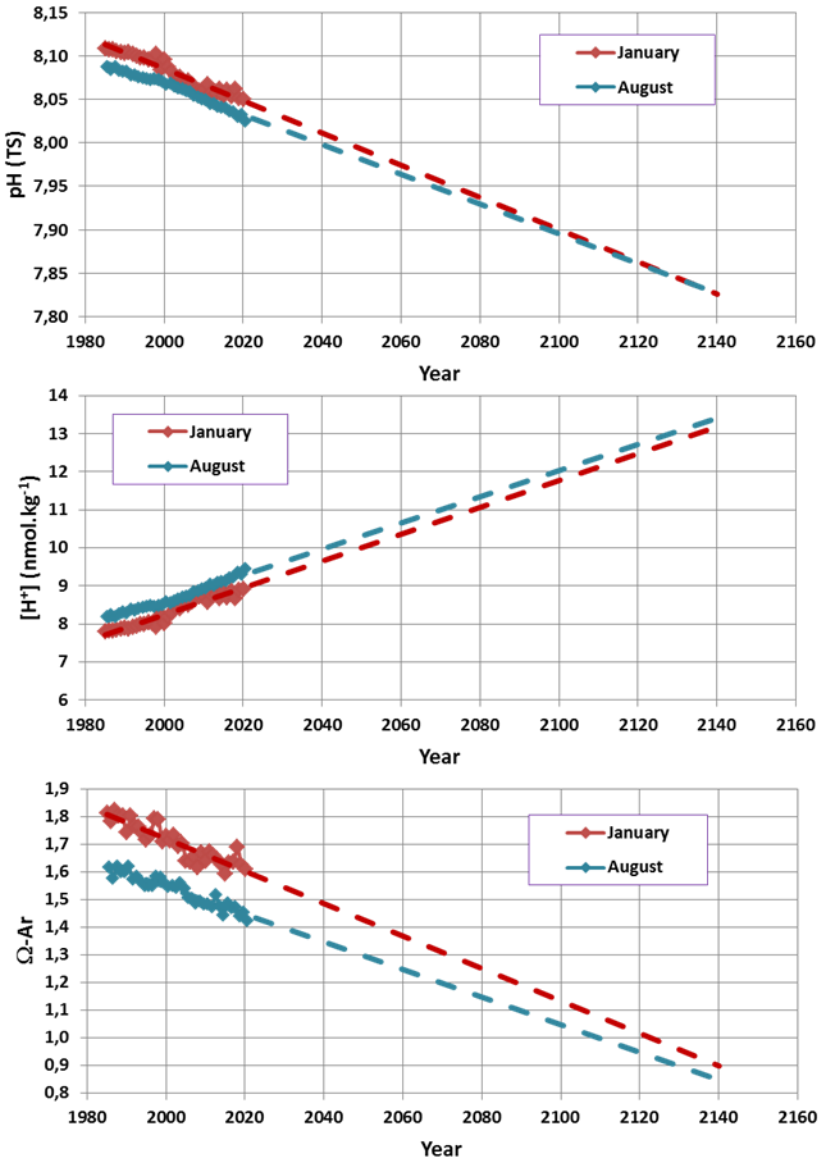

Figure S18: Evolution of sea surface fCO_2 (µatm), pH (TS), $[CO_3^{2-}]$(µmol.kg^{-1}), $[H^+]$ (nmol.kg^{-1}), Ω_{Ar} and Ω_{Ca} in 1960-2110 evaluated for SSP5-8.5 scenarios for winter (blue line) taking into account both A_T and SST trends (same as Figure 15 in the main text). Here, results are also presented for the low and high C_T range (grey lines) based on error associated to the C_{ant} reconstruction.